J. Phys. II France 7 (1997) 1693–1707 NOVEMBER 1997, PAGE 1693

Effect of a Strong Electric Field on the Reentrant Nematic to Smectic A_d Phase Transition

Geetha Basappa ([1]), A.S. Govind ([1,2]) and N.V. Madhusudana ([1,*])

([1]) Raman Research Institute, C.V Raman Avenue, Bangalore 560 080. India
([2]) Department of Physics, Vijaya College, Basavanagudi, Bangalore 560 004, India

(Received 27 February 1997, revised 20 May 1997, accepted 3 July 1997)

PACS.61.30.Gd – Orientational order of liquid crystals: electric and magnetic field effects on order
PACS.64.70.Md – Transitions in liquid crystals

Abstract. — We report experimental studies on the effect of a strong electric field on the nematic-smectic A_d ($N-A_d$) and A_d-reentrant nematic (A_d-N_R) phase transitions in a binary mixture. Both the transition temperatures increase with field. The A_d-N_R transition point changes much more rapidly than that of A_d–N transition, indicating that the A_d phase will get bounded at a sufficiently high field. We have included the effect of the electric field in our molecular model of reentrant phases in highly polar compounds, in which the mutual orientation of near neighbour molecules changes from an antiparallel to a parallel configuration as the temperature is lowered. It is argued that the cross-over temperature increases with field which accounts for the observed trends. For suitable parameters, it is also predicted that either a nematic-nematic transition line can branch off from the A_d-N_R line or a smectic A–smectic A transition line can meet the A_d-N_R line at an appropriate field. In the latter case, the A_d-N_R line has an associated slope change which is consistent with the experimental data.

1. Introduction

Many mesomorphic compounds exhibit both nematic (N) and smectic A (S_A) phases. The N phase breaks the rotational symmetry of the isotropic phase and has a long range orientational order of rod like molecules [1,2]. The S_A phase has an additional translational order along the director **n**, which is a unit vector representing the average orientation direction of the molecules. Thus the S_A phase breaks the translational symmetry of the N phase along **n**. In view of the lower symmetry of the S_A phase, it usually occurs at lower temperatures compared to the N phase. However, it is now well-established that in compounds whose molecules have strongly polar cyano or nitro end groups, the nematic phase can reenter, as the S_A liquid crystal is cooled to a low enough temperature [1–3]. It is also established that the S_A phase which occurs between the higher temperature N phase and the lower temperature reentrant nematic (N_R) phase is characterized by a layer spacing d which is somewhat longer than the molecular length. This S_A phase with such a "partial bilayer" structure is called the A_d phase and arises due to an antiparallel orientation between neighbouring polar molecules [4,5] such that the aromatic

(*) Author for correspondence (e-mail: nvmadhu@rri.ernet.in)

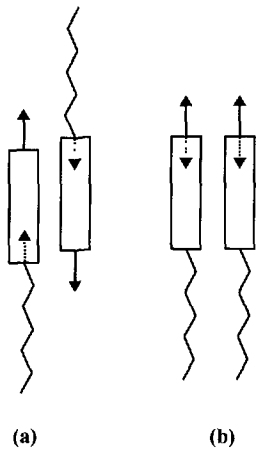

Fig. 1. — Schematic diagram showing the mutual configuration in an antiparallel (a) and a parallel (b) pair of polar molecules. The arrow head at the end of the solid line indicates the permanent dipole at the end of the molecule. The one with the dotted line is the dipole induced by the permanent dipole of the neighbouring molecule.

cores overlap. Highly polar compounds also exhibit many other interesting phase sequences like double reentrance with a "monolayer" smectic A_1 phase occurring at temperatures lower than the stability range of the N_R phase, smectic A polymorphism, occurrence of a reentrant nematic lake surrounded by the S_A phase in binary mixtures, *etc.* [1]. All these phenomena have been successfully described by the Landau theory with two coupled smectic order parameters developed by Prost *et al.* [6]. The two order parameters correspond to the molecular length l and the length of the partial bilayer structure d mentioned above.

Another simple way of describing the reentrant nematic phase is to construct a Landau theory in which the orientational and translational order parameters are appropriately coupled. Following an argument of McMillan [7], de Gennes incorporated the lowest order coupling between the two order parameters which will enhance the bare S_A–N transition point [1]. A reentrant nematic phase can be obtained by introducing a higher order coupling which destabilizes the smectic order when the orientational order is large [8]. The effect of an electric field (E) on the S_A–N_R transition has been worked out by Lelidis and Durand [8] who have shown that this transition point increases with E.

There have also been several attempts to develop molecular theories of the above phenomena. In particular, Berker *et al.* [9,10] have developed a frustrated spin gas model in which triplets of polar molecules are considered to be the basic units and different internal configurations of these units give rise to the different phases mentioned above. In this model it is assumed that the orientational order is saturated in all the phases ($S = 1$). Guillon and Skoulios [11], have argued that the amphiphilic character of the molecules can give rise to a mixture of head to head dimers and individual molecules in the A_d phase. The possibility of reentrance due to steric interaction of the chains has been pointed out by these authors.

The interaction between permanent dipoles favours an antiparallel orientation (A) between neighbouring molecules. This interaction energy is $\propto 1/r^3$ where r is the intermolecular separation. The strongest intermolecular interaction arises from the anisotropic dispersion energy between the aromatic cores resulting in the partial bilayer structure mentioned earlier (Fig. 1a). If the polar molecules are parallel, the dipolar interaction is repulsive. However, in view of the strong polarisability of the conjugated aromatic core to which the dipole is attached, the latter

induces an oppositely oriented dipole moment in the neighbouring molecule thus reducing the net dipole moment of each molecule (Fig. 1b). Further, in this "parallel" or (P) configuration, the chains are in close proximity, adding to the attractive interaction. Both these effects are $\propto 1/r^6$. Hence, as the density is increased *i.e.*, the temperature is lowered, one can expect a change in the configuration of the pairs from "A" type to "P" type. The two configurations shown in Figure 1 naturally account for the two length scales in the Landau theory developed by Prost [6]. The McMillan parameter which is a measure of the smectic interaction potential is larger for the "A" type of pairs compared to that for the "P" type of pairs. A molecular theory of double reentrance has been developed using these ideas [12]. We have recently extended this model to account for other phenomena exhibited by polar compounds like smectic polymorphism, nematic lake *etc.*, [13].

All the compounds which exhibit the N_R phase are highly polar and as such an external electric field (E) can have a very strong influence on the orientational order of these compounds. This can in turn influence both the N–A_d and A_d–N_R phase transition temperatures. Indeed as E^2 is conjugate to the orientational order of the medium, the nematic to field induced paranematic transition exhibits a critical point at an appropriate field. Experimental studies on electric field effects are hampered by the inevitable Joule heating of the sample due to the ionic currents and dielectric heating due to the relaxation of molecular dipoles at a relatively low frequency. Recently, Durand *et al.* [14, 15] have quantitatively studied the critical point in the nematic phase by using short pulses of electric fields separated by a long time interval to allow the system to remain in thermal equilibrium. More recently, we have developed an alternative experimental technique in which the *local* temperature of the sample is monitored to take account of the heating effect [16].

In this paper, we present our results on the electric field phase diagram of a mixture exhibiting both N–A_d and A_d–N_R phase transitions. It has been obtained using an improved experimental technique (Sect. 2). The N–A_d transition temperature increases moderately with field. On the other hand the A_d–N_R transition temperature increases rapidly with field indicating that the A_d phase can be bounded in the phase diagram. We have not been able to apply a high enough field to confirm this in the present case.

In Section 3, we have extended our molecular theory to include the effect of an electric field on the phase diagram. Depending on the parameters used, we get either a weak increase or decrease of N–A_d transition point with the field. The A_d–N_R transition point has a large increase with the field and the A_d phase is bounded. The parameter set can also be chosen to get a field induced first order nematic-nematic transition line which branches off from the A_d–N_R line. The two nematic phases differ in the nature of the short range order (*i.e.* relative number of parallel and antiparallel pairs referred to earlier). Another possibility is that an S_A–S_A transition line which occurs for a similar reason, can meet the A_d–N_R line at an appropriate field. This would produce a change in the slope of the latter which appears to be consistent with our experimental results.

We end with some conclusions in Section 4.

2. Experimental Technique and Results

An external electric field couples to the dielectric anisotropy of the liquid crystal and can hence alter its orientational order parameter. The orientational part of the free energy density due to the field is given by:

$$F_E = -\frac{\Delta\epsilon_1}{12\pi} E^2 S \tag{1}$$

where S is the orientational order parameter and $\Delta\epsilon_1$ is the dielectric anisotropy of the medium with $S = 1$. Typically $\Delta\epsilon_1 \sim 20$ and if the field induced shift in the nematic-paranematic

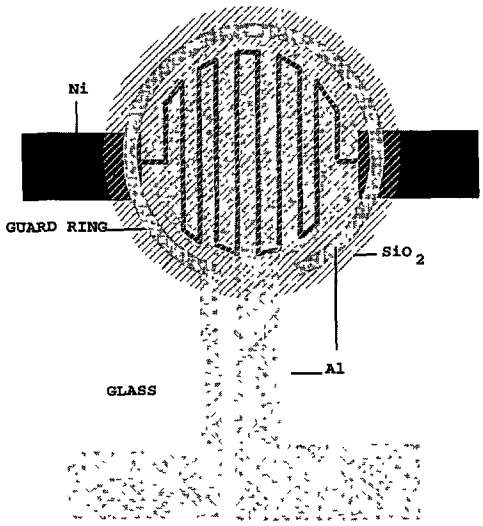

Fig. 2. — Schematic diagram indicating the geometric disposition of the nickel thermometer, SiO_2 insulator and the aluminium electrode on the lower plate of the cell.

transition point is ~ 1 K, the field energy should be $\sim 0.01 k_B T_{NI}$ or $E \sim 10^5$ V/cm. The organic compounds used in such experiments always have residual ionic impurities which dissipate energy by flow when the field is applied. To avoid electrode polarization, an AC electric field at a frequency of a few kHz is used in the experiments. The polar compounds have a relaxation of $\epsilon_{//}$, the dielectric constant parallel to the director **n** at frequencies ~ 1 MHz. The effect of this relaxation is felt even when the frequency of the applied voltage is a few kHz, and causes dielectric heating in the sample [17]. When the field is applied continuously, the heating can increase the sample temperature by a few degrees, and mask the electric field effect on the transition temperatures mentioned earlier.

2.1. Experimental Technique. — We have recently developed a technique in which the *local* temperature of the sample subjected to a strong electric field is measured using an evaporated nickel film which is appropriately patterned [16]. This film is covered with an insulating silicon monoxide layer on which an aluminium electrode is evaporated. The counter electrode is etched on an indium-tin oxide ITO coated plate. Both the plates are treated with octadecyltriethoxysilane (ODSE) to get a homeotropic alignment of the liquid crystal. The sample thickness is typically ~ 20 μm and has been measured just outside the periphery of the electrode by an interferometric technique. In our earlier experiments, we had used unguarded electrodes which in view of the heating of the sample under the field, could result in a temperature gradient near the edge of the electrode. To minimize the errors due to this, we have redesigned the aluminium electrode by incorporating a "guard ring" around it (Fig. 2). The electric field is applied to both the guard ring and the central electrode but only the central part is used in the electrical impedance analysis of the cell. We had used sinusoidal voltages in our earlier studies. As the orientational order parameter relaxation time is expected to be relatively short compared to the inverse frequencies used, this could lead to a nonlinear response of the system which itself is of interest [18]. In the experiments to be reported in this paper, we apply a square wave voltage to the sample to avoid the nonlinear response. The block

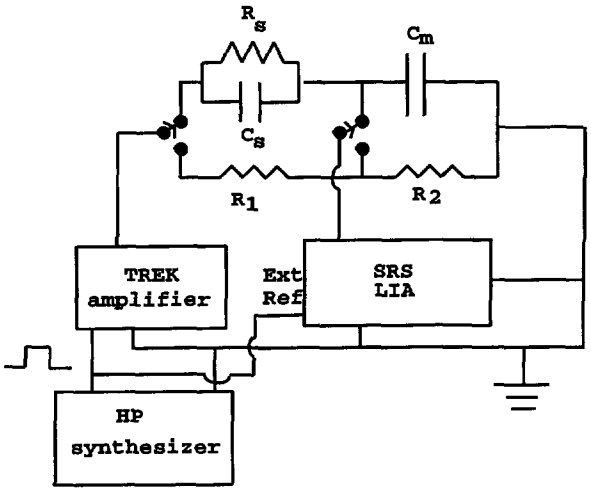

Fig. 3. — Block diagram of the circuit used for the electrical impedance measurement of the cell.

diagram of the electrical circuit is shown in Figure 3. The square wave voltage from an HP 3326A oscillator is amplified by a TREK 601 B amplifier and the output voltage V_A is applied to the cell. The current flowing through the cell is measured across a 0.9 μF series capacitor (C_m). The amplitude and phase of the amplified voltage applied to the cell are calibrated by measuring the voltage drop across a standard resistor R_2 in series with R_1 (see Fig. 3). The amplitude and phase of the output signal are measured using an SRS 830 lock-in amplifier. Both the capacitance C_s and resistance R_s of the sample are determined by an impedance analysis of the cell [16]. The capacitance is used to determine the dielectric constant $\epsilon_{//}$. The cell is mounted in an Instec HS1 hot stage and the entire experiment is controlled by a PC.

In some of the experimental runs, we found it difficult to detect the N–A_d and A_d–N_R transitions using the electrical parameters of the cell as both $\epsilon_{//}$ and the conductivity $\sigma_{//}$ varied relatively smoothly across the transitions. Hence we used a simple light scattering technique to detect the transitions. For this purpose, the hot stage was fixed on a platform which itself was mounted on the rotating stage of Leitz polarising microscope (model Orthoplan) used in the reflection mode (Fig. 4). The orientation of the platform could be adjusted using leveling screws. A polarized He-Ne laser beam was chopped at 171 Hz and allowed to be incident on the sample through the upper transparent ITO electrode of the cell. The beam was reflected by the lower aluminium electrode. The reflected beam was cut off using an analyser and the back scattered light was collected using an INTEVAC intensified photodetector which has a relatively large cathode area. The output was monitored using a lock-in amplifier (Fig. 4). In this geometry, we measure the scattered intensity due to twist fluctuations in the sample. These fluctuations are not allowed in the smectic A phase and hence the N–S_A transition is characterized by a rapid fall in the scattered intensity [1].

As we mentioned earlier, the *local* temperature of the sample was measured using a nickel thermometer. The resistance of the nickel film was measured using a four probe technique using a Keithley 2000 multimeter. It was calibrated using an appropriate procedure with reference to the INSTEC hot stage temperature. The calibration was periodically checked during the experiment.

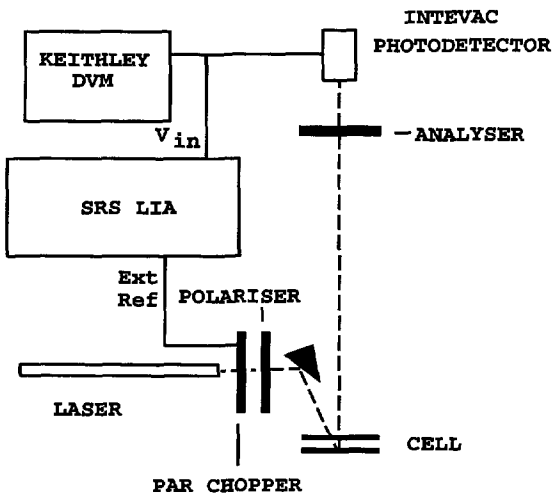

Fig. 4. — Schematic diagram of the optical set up used to measure the scattered intensity. The dotted line indicates the light beam. The angle of reflection from the prism and the cell are highly exaggerated for the sake of clarity.

2.2. Experimental Procedure and Results. — Mixtures of hexyloxy cyano-biphenyl (6OCB) and octyloxy cyanobiphenyl (8OCB) exhibit the phase sequence isotropic–N–A_d–N_R over a wide range of compositions. As the N–A_d and A_d–N_R transitions occur at relatively low temperatures, mixtures of these compounds have been studied extensively [19–21]. For our studies we have chosen a specific mixture with 27 wt% of 6OCB. The pure compounds were obtained from Aldrich. The mixture has the following sequence of transitions:

$$\text{Isotropic} \overset{78.3\ ^\circ\text{C}}{\longrightarrow} \text{N} \overset{47.2\ ^\circ\text{C}}{\longrightarrow} \text{A}_\text{d} \overset{28.4\ ^\circ\text{C}}{\longrightarrow} \text{N}_\text{R}.$$

All the experimental runs were taken while cooling the sample. The field free transition points were located using the light scattering experiment (Fig. 5). As the same lock-in amplifier was used for both light scattering and dielectric measurements, these runs were independent of each other. The temperature was lowered in steps of $\sim$ 0.08 °C and the data were collected after waiting for a few minutes for stabilization of temperature. As the applied field is increased, the thermal fluctuations of the director are quenched in the nematic phase and hence the scattered intensity is reduced. However, we can still see a change of slope of the scattered intensity even at the highest fields used in the experiment, which has been used for locating the relevant transition point.

The temperature variation of the dielectric constant $\epsilon_{//}$ in the N_R phase has a steeper slope compared to that in the S_{Ad} phase. This is in agreement with some earlier studies on the same system [20]. We have used this fact to locate the A_d–N_R transition temperature in a few runs. In other runs the change in slope was not sharp enough to locate the transition temperature unequivocally using this technique.

As we have discussed in our earlier paper [16], in pure 8OCB, the N–A_d transition could be clearly detected because of a small but sharp decrease in R_s at the transition point. Though the permeation effect in the A_d phase could be expected to produce the opposite effect, as we argued in [16], the sharp decrease in the relaxation frequency of $\epsilon_{//}$ which contributes to the conductivity even at the frequency of measurement, would lead to the observed trend.

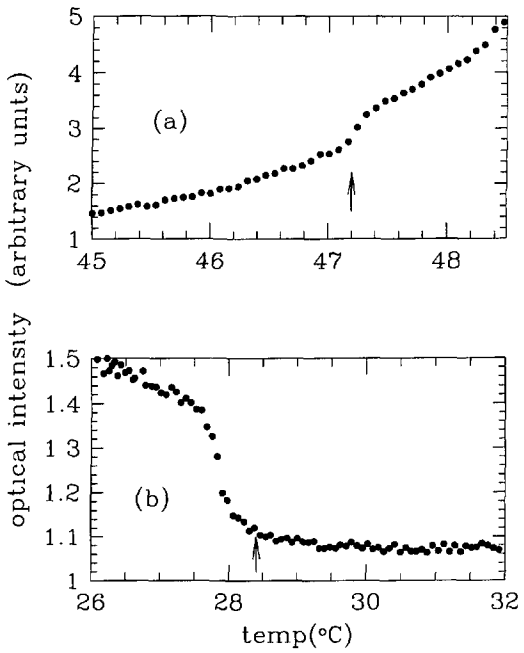

Fig. 5. — Intensity of scattered light as a function of temperature for $V = 0$ (a) near the A_d-N transition point and (b) near the A_d-N_R transition point (transition temperatures indicated by arrows).

As in the case of the dielectric data the resistance measurements were used to locate the transition temperature in those cases in which the signature was unambiguous. We found that the temperatures agreed with the optical measurements to about ± 0.5 °C for the A_d-N_R transition point. As all the experiments are conducted while cooling the sample the scatter in the data may partly arise from different extents of supercooling of the sample. The agreement between the two independent types of measurements is better for the $N-A_d$ transition, ($\sim \pm 0.2$ °C). The field free N_R-A_d and A_d-N transition points were checked before the start of the experiment, and after it was completed, and were found to be constant to within ±0.2 °C, which is less than the uncertainty in locating the A_d-N_R transition temperature using different techniques.

Both the A_d-N_R and A_d-N transition temperatures increase with field though the variation of the former is much stronger than that of the latter. We have applied voltages up to 300 V (at 4111 Hz) on a sample with thickness $\sim$ 20 μm to construct the phase diagram shown in Figure 6. Though we have shown the field dependence of the A_d-N_R transition temperature by a smooth line as a guide to the eye note that the data is consistent with a change of slope at $\sim$ 200 esu. In the next section we present a theoretical model which describes the electric field phase diagram.

3. Molecular Model

3.1. ASSUMPTIONS. — In the following, we extend our molecular theory of highly polar compounds [12, 13] to include the effect of a strong electric field. In order to simplify the calculations, the following assumptions, which are discussed elsewhere in detail [12, 13], have been made.

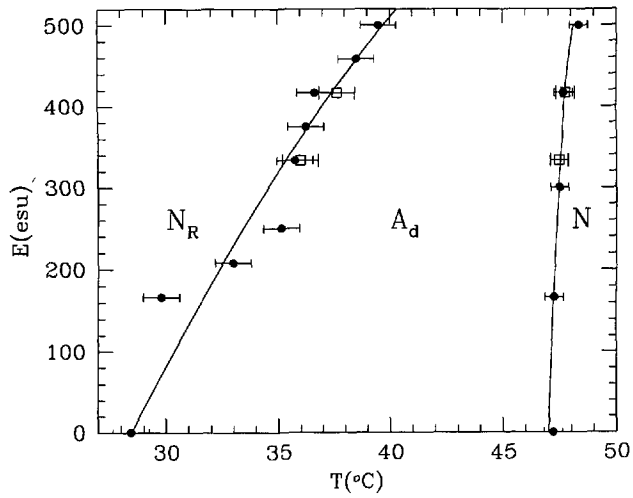

Fig. 6. — The electric field phase diagram for the 6OCB - 8OCB mixture. Circles are data obtained from light scattering measurements and open squares are those obtained from the electrical impedance measurements. The solid lines are guides to the eye. Note that the data on the $N_R - A_d$ transition are consistent with a change of slope at 200 esu.

(1) As described in the Introduction the medium is assumed to consist of "pairs" of molecules having either antiparallel (A) or parallel (P) configurations. Frustration in the orientation of a third molecule can lead to stable pairs with A–type of configuration. On the other hand, a large number of molecules can be associated in the P–type configuration. However, for the sake of simplicity, we assume that even the P–type configuration consists of only pairs, as in the earlier papers.

As we described earlier, the A–type (P–type) configuration is favoured at lower (higher) densities. Again, for the sake of simplicity, it is assumed that the energy difference between the two configurations has the following form:

$$\Delta\mathcal{E} = \mathcal{E}_A - \mathcal{E}_P = R_1 k_B T_{NI} \left(\frac{R_2}{T_R} - 1 \right) \tag{2}$$

where k_B is the Boltzmann constant, $\mathcal{E}_A$ and $\mathcal{E}_P$ are the configurational energies of the A–type and P–type pairs respectively, T_{NI} is the nematic-isotropic transition temperature of the A–type of pairs, $R_1 k_B T_{NI}$ is an interaction parameter and $T_R = T/T_{NI}$ is the reduced temperature. R_2 is the reduced temperature at which the density of the medium is such that $\Delta\mathcal{E}$ becomes zero. For $T_R > R_2$, the A–type configuration has the lower energy. R_2 can be expected to depend weakly on the chain length in a homologous series *i.e.*, on the McMillan parameter α. We ignore this dependence of R_2 on α.

(2) Since the A and P type of pairs are geometrically dissimilar, we assume that the orientational potential for A–type of pairs (U_{AA}) and P–type of pairs (U_{PP}) to be different. We write, as in [22]

$$U_{PP} = Y U_{AA} \tag{3}$$

and the mutual interaction potential

$$U_{AP} = U_{PA} = Q\sqrt{U_{AA} U_{PP}} \tag{4}$$

where $Q \neq 1$ indicates a deviation from the Geometric Mean (GM) rule in the orientational potential. The McMillan parameters [7] for A–type (α_A) and P–type (α_P) configurations can

be written as

$$\alpha_{\mathrm{A}} = 2\exp\left(-[\pi r_{\mathrm{o}}/(r_{\mathrm{o}}+2c)]^2\right) \tag{5}$$

and

$$\alpha_{\mathrm{P}} = 2\exp\left(-[\pi r_{\mathrm{o}}/(r_{\mathrm{o}}+c)]^2\right) \tag{6}$$

where r_{o} and c are the lengths of the aromatic and chain moieties of the molecule respectively. α_{P} is obviously related to α_{A}. The mutual interaction parameter

$$\alpha_{\mathrm{PA}} = \alpha_{\mathrm{AP}} = \alpha_{\mathrm{E}} = Q'\sqrt{\alpha_{\mathrm{A}}\alpha_{\mathrm{P}}} \tag{7}$$

where $Q' \neq 1$ indicates a deviation from the geometric mean rule in the smectic interaction.

(3) Following Kvenstel *et al.*, [23] we decouple the translational and orientational parts in the McMillan's "mixed" order parameter (σ) and as in [12] we write

$$\langle P_2\cos(\theta)\cos(2\pi Z/d)\rangle \;=\; \langle P_2(\cos\theta)\rangle\langle\cos(2\pi Z/d)\rangle \tag{8}$$

i.e., $\sigma = S\,\tau$ where $\langle\rangle$ indicate a statistical average, $P_2(\cos\theta)$ is the second Legendre polynomial, θ being the angle made by the molecular long axis with the director, Z the coordinate of the molecular center along the direction of layer normal, d the layer thickness. S and τ the nematic and the smectic order parameters respectively.

(4) The electric field can in general be expected to enhance the density of the medium (electrostriction). The "direct" effect arises from the pressure due to the field, $\Pi_E = \epsilon_{//}E^2/(8\pi)$ and yields $\delta\rho/\rho = \kappa_T\epsilon_{//}E^2/(8\pi)$, where κ_T is the isothermal compressibility. For the highest field that we apply, $\delta\rho/\rho \sim 10^{-5}$ However, as we mentioned, the anisotropy of dielectric constant couples to the field to enhance the order parameter of the medium. This results in another contribution to the electrostriction:

$$\delta\rho = \left[\frac{\partial\rho}{\partial S}\right]_T \delta S(E) \tag{9}$$

with

$$\delta S(E) \simeq \frac{\chi\Delta\epsilon_1 E^2}{24\pi} \tag{10}$$

where χ is the susceptibility for the orientational order and is assumed to be $\sim 5\times10^{-8}$ in the present calculations. Horn [24] has measured the order parameter of pentyl cyanobiphenyl as a function of pressure and at temperatures much lower than T_{NI}, $[\partial\rho/\partial S]_T$, $\simeq 0.3$. Using these values, $\delta\rho/\rho$ at the highest fields used $\sim 2\times10^{-3}$, which is 200 times larger than the direct electrostriction effect estimated earlier. Hence the intermolecular separation decreases with E^2, and this can in turn be expected to change R_2. In view of the above discussions, we can write:

$$R_2(E) = R_2(0) + CE^2. \tag{11}$$

C is estimated from our earlier calculation [12] of the variation of $\Delta\mathcal{E}$ given by equation (2) with r the intermolecular separation and is found to be $\simeq 10^{-8}$ cgs units. We have not taken into account the possible volume-dependence of the orientational and layering potentials, the affect of which will be much smaller than the one discussed above.

In order to calculate the enhancement due to the field in the orientational order parameter in the context of a molecular model, it is necessary to use the orienting effect of the field on the dipole moments as well as the anisotropic polarizabilities of the molecules. For the sake

of simplicity, we assume that due to the field both the A and P type pairs have an orienting potential of the form,

$$U_{\mathrm{A}}(E) = -\beta_{\mathrm{A}} E^2 \cos^2\theta_{\mathrm{A}}$$

and

$$U_{\mathrm{P}}(E) = -\beta_{\mathrm{P}} E^2 \cos^2\theta_{\mathrm{P}} \tag{12}$$

where β_{A} and β_{P} can be estimated from the known dielectric anisotropy. We get $\beta_{\mathrm{A}} \simeq 1000/N$ cgs units where N is the Avogadro number. It is known from dielectric studies [20] that the dielectric anisotropy for the $\mathrm{N_R}$ phase in which the P–type of pairs dominate is $\sim 10\%$ higher than that for the $\mathrm{A_d}$–phase in which the A type pairs dominate. As such, we use $\beta_{\mathrm{P}} \simeq 1.1\ \beta_{\mathrm{A}}$.

3.2. Free Energy and Order Parameters. — The medium is assumed to consist of a *mixture* of A–type pairs and P–type pairs. Extending the McMillan theory for mixtures, the potential energy of the ith A–type of pair in the absence of electric field can be written as

$$\begin{aligned} U_{\mathrm{Ai}} = & - U_{\mathrm{AA}} X_{\mathrm{A}} S_{\mathrm{A}} P_2(\cos\theta_{\mathrm{Ai}})[1 + \alpha_{\mathrm{A}}\tau_{\mathrm{A}} \cos(2\pi Z_{\mathrm{i}}/d)_{\mathrm{A}}] \\ & - U_{\mathrm{AP}} X_{\mathrm{P}} S_{\mathrm{P}} P_2(\cos\theta_{\mathrm{Ai}})[1 + \alpha_{\mathrm{AP}}\tau_{\mathrm{P}} \cos(2\pi Z_{\mathrm{i}}/d)_{\mathrm{A}}] \end{aligned} \tag{13}$$

where X_{A}, X_{P}, $S_{\mathrm{A}}, S_{\mathrm{P}}$ and τ_{A}, τ_{P} are the molefractions, orientational and translational order parameters of A and P type of pairs respectively. Similarly for a P–type pair, U_{Pj} is obtained by interchanging suffixes A and P in equation (13). Now, the internal energy of one mole of pairs in the presence of electric field can be written as

$$\begin{aligned} 2U = & \frac{NX_{\mathrm{A}}}{2}\langle U_{\mathrm{Ai}}\rangle + \frac{NX_{\mathrm{P}}}{2}\langle U_{\mathrm{Pj}}\rangle - NX_{\mathrm{P}}\Delta\mathcal{E} \\ & -N(X_{\mathrm{A}}\beta_{\mathrm{A}}\langle\cos^2\theta_{\mathrm{Ai}}\rangle + X_{\mathrm{P}}\beta_{\mathrm{P}}\langle\cos^2\theta_{\mathrm{Pj}}\rangle)E^2 \end{aligned} \tag{14}$$

where the factor 2 on the left hand side reminds us that we have a mole of pairs and we have also added the concentration dependent part of the configurational energy.

The molar entropy is given by:

$$\begin{aligned} 2S = & - Nk_{\mathrm{B}}[X_{\mathrm{A}} \int f_{\mathrm{Ai}} \ln f_{\mathrm{Ai}}\ \mathrm{d}(\cos\theta_{\mathrm{Ai}})\ \mathrm{d}Z_{\mathrm{Ai}} + X_{\mathrm{P}} \int f_{\mathrm{Pj}} \ln f_{\mathrm{Pj}}\ \mathrm{d}(\cos\theta_{\mathrm{Pj}})\mathrm{d}Z_{\mathrm{Pj}}] \\ & - Nk_{\mathrm{B}}(X_{\mathrm{A}} \ln X_{\mathrm{A}} + X_{\mathrm{P}} \ln X_{\mathrm{P}}) \end{aligned} \tag{15}$$

where the last term is the entropy of mixing and f_{A} and f_{P} are the distribution functions of A and P type of pairs respectively. The Helmholtz free energy is given by:

$$F = U - TS. \tag{16}$$

The distribution functions f_{A} and f_{P} are found by minimizing F. We can show that the decoupling assumption (see Eq. (8)) leads to the result

$$f_{\mathrm{A}} = f_{\mathrm{Ao}} f_{\mathrm{At}}, \text{and } f_{\mathrm{P}} = f_{\mathrm{Po}} f_{\mathrm{Pt}} \tag{17}$$

where f_{Ao} and f_{At} are the orientational and translational distribution functions of the A–type of pairs and f_{Po} and f_{Pt} are similar functions for P–type of pairs.

Hence the order parameters are given by:

$$S_A = \int_0^1 P_2(\cos\theta_{Ai}) f_{Ao} d(\cos\theta_{Ai}) \tag{18}$$

and

$$\tau_A = \int_0^1 \cos(\pi Z') f_{At} dZ' \tag{19}$$

where the reduced co-ordinate $Z' = (2Z_i/d)_A$ is used. S_P and τ_P are obtained by interchanging the suffixes A and P in equations (18) and (19). The equilibrium value of molefraction X_A of the A–type of pairs is found by minimizing F with respect to X_A.

3.3. CALCULATIONS. — Calculations have been made for $R_2 = 0.8$ and 0.6 with $R_1 = 15$ and 6 which are very reasonable values [12]. We evaluate all the necessary integrals using a 32 point Gaussian quadrature method in double precision.

We look for the following types of solutions:

1) $S_A, S_P \neq 0$, $\tau_A = \tau_P = 0$ leading to nematic phase which is N_1 if X_A is small and N_d if X_A is large. and;

2) $S_A, S_P \neq 0$, $\tau_A, \tau_P \neq 0$ leading to the smectic phase which is S_{A1} if X_A is small and S_{Ad} if X_A is large.

3.4. RESULTS AND DISCUSSION. — We first consider the simplest case in which $Q = Q' = 1$, *i.e.*, the geometric mean rule is assumed to be valid and further $Y = 1$, *i.e.*, the orientational potentials for both A and P types of pairs are equal. As we have shown elsewhere [12], with $R_1 = 15$, $R_2 = 0.8$ and $\alpha_A = 1$, we can get a double re-entrant sequence, *viz.*, $N-A_d-N_R-A_1$, as the temperature is lowered. With $C = 10^{-8}$ cgs units as estimated after equation (11), we have calculated the effect of electric field on the $N-A_d$ and A_d-N_R transition temperatures. The results are shown in Figure 7. The A_d range in the absence of E is relatively large (~ 90 °C) compared to that of our experimental system. However, both the $N-A_d$ and A_d-N_R transition temperatures increase with field at low fields. The lower transition temperature increases more rapidly than the upper one. As the field is increased beyond some value, the $N-A_d$ transition temperature actually starts to *decrease*. This would imply that for a large enough field, the A_d phase can disappear.

Indeed if we reduce R_1 to 6 and α_A to 0.96, we get the phase diagram shown in Figure 8. In this case the A_d range is $\simeq 30$ °C when $E = 0$. The $N-A_d$ transition temperature decreases with field even at low fields and the A_d phase is bounded. Beyond an electric field ~ 650 esu there is no A_d phase.

We have calculated the electric field phase diagrams with other possible parameter sets. The geometric mean rule is usually not satisfied in actual mixtures of nematogens [25] and usually, $Q < 1$. Further, the orientational potential of the two types of pairs can be different, *i.e.*, $Y \neq 1$ in general. As we have described earlier, the P–type configuration need not be confined to pairs and hence the effective orientational potential can be higher for the P–type of "pairs" than for the A–type *i.e.*, $Y > 1$. We have calculated the effect of an electric field by assuming the following set of parameters: $R_1 = 15$, $R_2 = 0.6$, $Q = 0.7935$, $Y = 2$ and $\alpha_A = 0.56$. The A_d range for $E = 0$ is ~ 25 °C in this case. Now as seen in Figure 9, a new feature develops in the phase diagram. At $E \sim 400$ esu, the A_d-N_R branch bifurcates showing an additional nematic-nematic transition at lower temperatures. We have indicated the two nematic liquid crystals which arise in the reentrant region by N_1 and N_d, which signify that N_1 has a higher

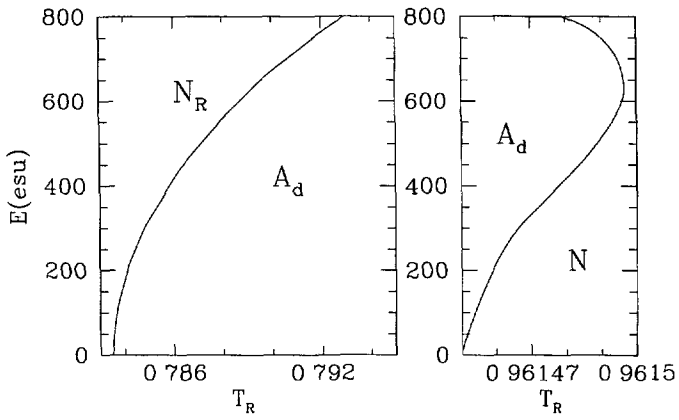

Fig. 7. — Calculated phase diagram showing N_R–A_d and A_d–N transition temperatures as functions of electric field E with $R_1 = 15$, $R_2 = 0.8$, $Q = Y = 1$, $\alpha_A = 1$ and $C = 10^{-8}$ cgs units. Note that the temperature scales are different for the two transitions.

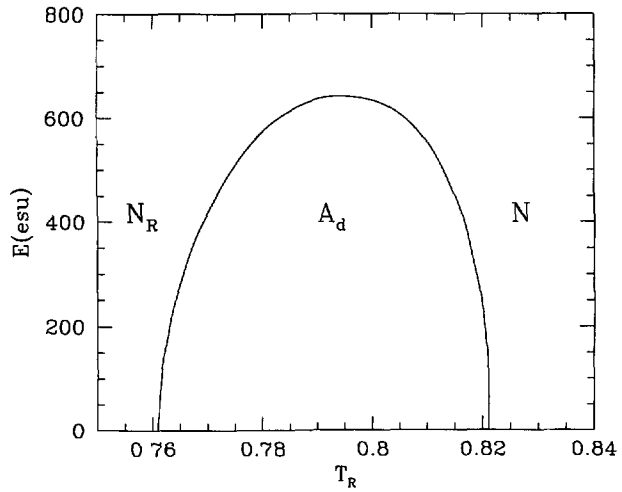

Fig. 8. — Calculated phase diagram showing bounded A_d region for $R_1 = 6$, $R_2 = 0.8$, $Q = Y = 1$, $\alpha_A = 0.96$ and $C = 10^{-8}$ cgs units.

concentration of P–type of pairs compared to the N_d phase. Above 400 esu A_d–N_R line varies more rapidly with field than at lower fields and the A_d phase is bounded. Indeed as we have discussed earlier [22] for parameters close to the ones assumed here, we get a nematic-nematic transition which is very weakly first order in nature, associated with a jump in X_A. As a function of either Q or Y, such a transition can end in a critical point at which X_A varies continuously. We expect that in the present case, the N_d–N_1 transition should end in a critical point as a function of field. The jump in X_A indeed decreases at higher fields, though we have not extended our calculations all the way to the critical point. (If the parameters are chosen as $R_1 = 15$, $R_2 = 0.8$, $Q = 0.71$, $Q' = 1$, and $Y = 1$ the N_1–N_d critical point occurs at $E \simeq 1125$ esu and at a temperature $T_R = 0.8980$.) As the jump in the orientational order parameter is rather small (~ 0.002 [22]), the N_1–N_d transition is difficult to detect except in

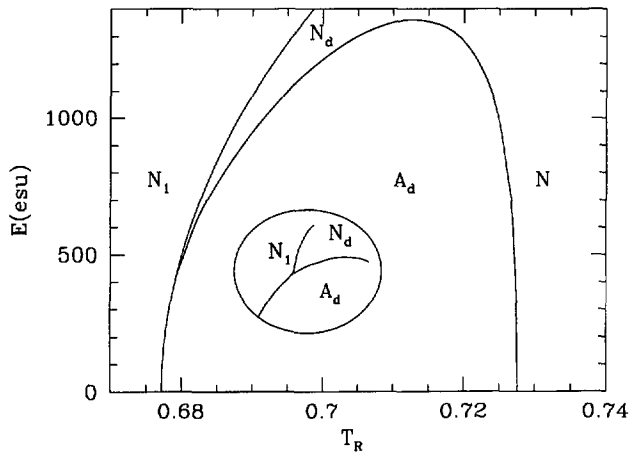

Fig. 9. — Calculated phase diagram showing the nematic-nematic line branching off from N_R–A_d line at $E \sim 360$ esu and $T_R \sim 0.68$, for $R_1 = 15$, $R_2 = 0.6$, $Q = 0.7135$, $Y = 2$, $\alpha_A = 0.56$ and $C = 10^{-8}$ cgs units. The inset shows an exaggerated topology near the branching point.

specific heat measurements. We can see from our experimental phase diagram (Fig. 6) that the change in the slope of the A_d–N_R line is opposite to the one shown in Figure 9. As such, it is unlikely that the possible change of slope is associated with the development of N_1–N_d transition.

In all the above calculations, the value of C in equation (11) was chosen on the basis of experimental data on 5CB. Our dielectric measurements on the 6OCB-8OCB mixture used in the experiment reported in this paper clearly indicate that the susceptibility χ has a value $\simeq 3 \times 10^{-7}$ near the N_R–A transition temperature. The larger value shows that the concentration of parallel pairs is relatively high in this mixture, compared to that in 5CB, as it should be for the occurrence of the reentrant nematic phase. Indeed in another compound which shows only a nematic phase but with a relatively large fraction of parallel pairs, χ has a similarly large value [18]. As such the effect of the electric field on R_2 is much stronger, and in the next calculation we assume that $C = 8 \times 10^{-8}$ cgs units in equation (11).

We can expect that the mutual smectic interactions can also deviate from the geometric mean rule. As we have shown elsewhere [13], even when the orientational order is assumed to be saturated, $Q' < 1$ leads to an A_1–A_d transition which is weakly first order in nature. We have made calculations on the influence of the electric field on the phase diagram for the following set of parameters: $R_1 = 15$, $R_2 = 0.6$, $Q' = 0.55$, $\alpha_A = 0.95$ and $Q = Y = 1$. In this case the A_1–A_d transition temperature is higher than the A_1–N_R transition temperature when $E = 0$ (Fig. 10). As the field is increased, the A_d–A_1 and A_1–N_R lines meet and at higher fields only an A_d–N_R transition is realized. The change of slope of the smectic to N_R transition line is now similar to that seen in the experimental diagram (Fig. 6). The slope of the N_R–A line is also very close to the experimental value. X-ray studies on the mixture used in our experiments have been conducted [19]. However, they are not accurate enough to have detected a smectic A to smectic A transition. It would be interesting to look for such a transition in the system investigated. We should however note that in view of the approximations made in developing the molecular model and in particular the mean field approach, quantitative agreement between the theoretical calculations and experimental data cannot be expected. The qualitative trends suggested by the theory however are likely to be correct.

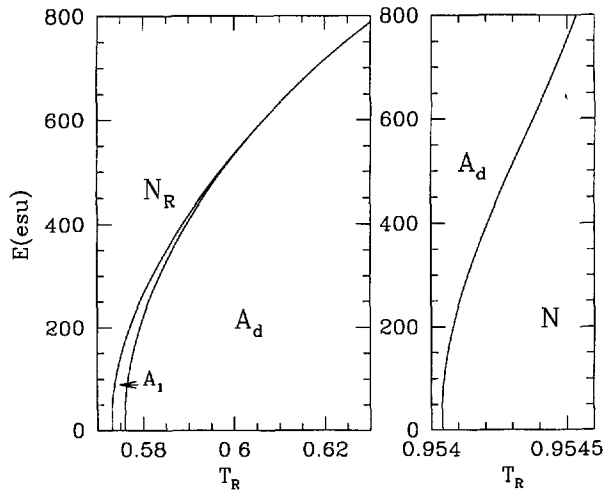

Fig. 10. — Calculated phase diagram showing the smectic-smectic line meeting the N_R–A_d line at $E \sim 600$ esu and $T_R \simeq 0.607$ for $R_1 = 15$, $R_2 = 0.6$, $Q = Y = 1$, $Q' = 0.55$, $\alpha_A = 0.95$ and $C = 8\times 10^{-8}$ cgs units. Note that the temperature scale for the A_d–N transition is different from that for the A_d–N_R transition.

As we have discussed elsewhere [13], in general, an increase of R_1 or α_A (chain length) increases the thermal range of the A_d phase. This trend can also be seen by comparing Figures 9 and 10. An increase of R_2 shifts both the A_d–N and A_d–N_R transition points to higher values. The N_1–N_d and A_1–A_d transitions become stronger if the deviations from the geometric mean rule in the orientational and layering potentials respectively are larger.

Our theoretical model gives rise to a rich variety of phase diagrams even in the absence of the field [13]. We are now calculating the effect of field on different types of phase diagrams predicted by the theory.

4. Conclusion

In conclusion, we have studied the electric field phase diagram of a liquid crystal mixture exhibiting a reentrant nematic phase. The temperature range of smectic phase is reduced as the field is increased. We have interpreted the phase diagram on the basis of a molecular theory of the reentrant phase proposed by us earlier, which predicts that the A_d phase gets bounded as the field is increased. This is reminiscent of a similar phase diagram as a function of pressure seen in many experiments [26]. On the basis of the molecular model, we can expect that R_2 will be an increasing function of pressure giving rise to the observed phase diagram. We have also shown on the basis of this model that a change of slope in the smectic-reentrant nematic transition line seen in our experiment may be caused by an underlying A_d–A_1 transition. Further experimental and theoretical studies on such systems are in progress.

Acknowledgments

We would like to thank Mr. H. Subramonyam for helping us in the preparation of the cells.

References

[1] de Gennes P.G. and Prost J., The Physics of Liquid Crystals, second edition (Clarendon, Oxford, 1993).
[2] Chandrasekhar S., Liquid Crystals, second edition, (Cambridge University Press 1992).
[3] Cladis P.E., *Phys. Rev. Lett.* **35** (1975) 48.
[4] Madhusudana N.V. and Chandrasekhar S., *Pramana Suppl.* **1** (1973) 57.
[5] Leadbetter A.J., Richardson R.M. and Colling C.N., *J. Phys. Colloq. France* **36** (1975) C1-37.
[6] Barois P., Pommier J. and Prost J., in Solitons in Liquid Crystals, Lui Lam and Jacques Prost, Eds. (Springer Verlag, 1991) p. 191 .
[7] McMillan W.L., *Phys. Rev. A* **6** (1972) 936.
[8] Lelidis I. and Durand G., *J. Phys II France* **6** (1996) 1359.
[9] Berker A.N. and Walker J.S., *Phys. Rev. Lett.* **47** (1981) 1469.
[10] Indekeu J.O. and Berker A.N., *J. Phys. France* **49**(1988) 353.
[11] Guillon D and Skoulios, A., *J. Phys. France* **45** (1984) 607.
[12] Madhusudana N.V. and Jyotsna Rajan, *Liq. Cryst.* **7** (1990) 31.
[13] Govind A.S. and Madhusudana N.V., *Liq. Cryst.*, in press.
[14] Lelidis I., Nobili M. and Durand G., *Phys. Rev. E* **48** (1993) 3818.
[15] Lelidis I. and Durand G., *Phys. Rev. E* **48** (1993) 3822.
[16] Basappa G. and Madhusudana N.V., *Mol. Cryst. Liq. Cryst.* **288** (1996) 161.
[17] Schadt M., *Mol. Cryst. Liq. Cryst.* **66** (1981) 319.
[18] Basappa G. and Madhusudana N.V., (to be published).
[19] Cladis P.E., *Mol. Cryst. Liq. Cryst.* **67** (1981) 177.
[20] Jadzyn J. and Czechowski., *Liq. Cryst.* **4** (1989) 157.
[21] Guillon D., Cladis P.E. and Stamatoff J., *Phys. Rev. Lett.* **41** (1978) 1598.
[22] Govind A.S. and Madhusudana N.V., *Liq. Cryst.* **14** (1993) 1539.
[23] Katriel J. and Kvenstel G.F., *Mol. Cryst. Liq. Cryst.* **124** (1985) 179.
[24] Horn R.G. and Faber T.E., *Proc. R. Soc. Lond.A.* **368** (1979) 199.
[25] Humphries R.L. and Luckhurst G.R., *Chem. Phys. Lett.* **23** (1973) 567.
[26] Kalkura A.N., Shashidhar R. and Urs M.S., *J. Phys. France* **44** (1983) 51.